Article published online: 2021-08-10

Effect of Surgical Design Variations on the Knee Contact Behavior during Anterior Cruciate Ligament Reconstruction

Malek Adouni, PhD[1,2] Tanvir Faisal, PhD[3] Yasin Dhaher, PhD[1,4,5,6]

[1] Department of Physical Medicine and Rehabilitation, Northwestern University, Chicago, Illinois
[2] Department of Mechanical Engineering, Australian College of Kuwait, Kuwait City, Kuwait
[3] Department of Bioengineering, University of Texas Southwest, Dallas, Texas
[4] Department of Mechanical Engineering, University of Louisiana at Lafayette, Louisiana
[5] Department of Physical Medicine and Rehabilitation, University of Texas Southwest, Dallas, Texas
[6] Department of Orthopedic Surgery, University of Texas Southwest, Dallas, Texas

Address for correspondence Malek Adouni, PhD, Department of Physical Medicine and Rehabilitation, Northwestern University, 710 N Lake Shore Dr, Chicago, IL 60611 (e-mail: malek.adouni@northwestern.edu; malek.adouni@polymtl.ca).

J Knee Surg 2023;36:310–321.

Abstract

In this study, we aimed to develop an in-silico synthesis of the effect of critical surgical design parameters on articular contact behavior for a bone-patellar-tendon-bone anterior cruciate ligament reconstruction (ACL-R) surgery. A previously developed finite element model of the knee joint consisting of all relevant soft tissues was employed. The knee model was further updated with additional features to develop the parametric FE model of the biomechanical experiments that depicted the ACL-R surgery. The parametricity was created involving femoral tunnel architecture (orientations and locations) and graft fixation characteristics (pretension and angle of fixation). A global sensitivity analysis based on variance decomposition was used to investigate the contribution of the surgical parameters to the uncertainty in response to the ACL-R joint. Our examinations indicated that the total contact force was primarily influenced by either combined or individual action of the graft pretension and fixation angle, with a modest contribution of the graft insertion sites. The joint contact center and area were affected mainly by the angle of fixation and the tunnel placements. Graft pretension played the dominant role in the maximum contact pressure variability, an observation that has been well-documented in the literature. Interestingly, the joint contact behavior was almost insensitive to the tunnel's coronal and sagittal orientations. Our data provide an evaluation of how the surgical parameters affect the knee joint's contact behavior after ACL-R and may provide additional information to better explain the occurrence of osteoarthritis as an aftermath of such surgery.

Keywords
- ACL reconstruction
- Surgical variability
- contact behavior
- finite element model

The anterior cruciate ligament (ACL) is an essential stabilizing soft tissue of a knee joint that is often the cause of traumatic injuries. Approximately 100,000 to 200,000 ACL ruptures occur each year in the United States.[1] The high rate of ACL injury explains the dramatic increase in the number of surgical reconstruction (ACL-R) procedures performed to

received
April 6, 2020
accepted after revision
June 21, 2021
article published online
August 10, 2021

Thieme Medical Publishers, Inc., 333 Seventh Avenue, 18th Floor, New York, NY 10001, USA

DOI https://doi.org/10.1055/s-0041-1733879.
ISSN 1538-8506.

avoid any secondary damage, thereby restoring the standard and high level of physical activity.[2,3] Although ACL-R provides short-term success in restoring stability and functional improvement, the procedure does not offer protection against early-onset joint degeneration and the development of osteoarthritis (OA) in the population with an ACL-reconstructed knee.[4] The earlier observation was confirmed by the high level of dissatisfaction, which reached 40%, and the high percentage (82 to 89%) of the degenerative radiographic changes observed within the treated population.[5–8] In addition to the associated defect due to initial trauma, in part, the initiation of OA may be attributed to the abnormal loading conditions of the reconstructed joint. The abnormal loading conditions may be mediated by surgical parameters such as single or double-bundle reconstruction, attachment sites, angle of fixation, graft pretension and tunnel orientations, or the patients' specific parameters such as postsurgical muscle activation patterns and joint geometry.[9,10] Despite the high correlation between the ACL-R treatment and posttraumatic knee OA, the exact etiology of this degenerative disease is not fully understood.[11]

Evidence indicates that the natural kinematics and kinetics of a knee joint are not restored following ACL-R with either a patellar tendon or hamstring tendon graft.[12–17] Furthermore, the loading conditions translated by contact behavior alterations, specifically on the articular cartilage, may impose a mechanical insult on areas that are not commonly loaded.[18] The new load distribution may lead to a more rapid degradation of the underlying tissue.[4,19] Surprisingly, the degree to which ACL-R affects the joint contact mechanics is not apparent yet. Indeed, except few published studies, the majority have not provided an accurate quantitative assessment of the essential variables of interest such as compartmental and total contact forces and areas as well as the distribution of stresses/strains.[20–25] Both experimental and computational studies focused on the effect of a limited number of surgical parameters such as the angle of flexion at the time of the graft fixation, the graft pretension, and the attachment sites on the joint's biomechanics under well-known clinical tests like Lachman and pivot tests.[14,19,22,24,26–32] The results reported in those studies have been characterized by significant discrepancies, due to the high variability of the surgical procedures and complexity of the interaction of the surgical parameters. However, the relative contributions of the surgical variables to the knee biomechanical response remain unclear; specifically, the tibiofemoral articular cartilages' contact response following an ACL-R.

In the current investigation, we adopted a systematic engineering approach to study the sensitivity of joint contact behavior to the surgical simulations of the bone-patellar-tendon-bone (BPTB) ACL-R procedure. The use of the sensitivity analysis framework is advantageous due to the multifactorial nature of the problem. A calibrated and validated healthy model and an ACL-R model[33–35] were used to identify the effect of the femoral tunnel's vertical and horizontal locations, femoral sagittal and coronal orientations, fixation angle and graft pretension on cartilage contact patterns, as estimated during isolated tasks (axial compression). Due to their correlation with cartilage degeneration and OA initiation,[36] the compartmental contact force and area, contact center location, and average and maximum contact stresses were considered as the output variables of interest.

Methods

Finite Elements Models and Simulations of the ACL-R Surgery

A previously developed computational model of the knee joint comprising all relevant soft tissues was employed in the present study.[35,37] The knee model includes three bony structures (tibia, femur, and patella) associated with the articular cartilage layers, menisci and the eight principal ligaments, anterior/posterior cruciate ligaments (ACL/PCL), medial/lateral collateral ligaments (LCL/MCL), medial/lateral patellofemoral ligaments (MPFL/LPFL), and patellar tendon and quadriceps ligament (PT/QL). The meshes of tibial, patellar and femoral articular cartilages as well as menisci were extensively refined. Furthermore, local elements' system axes were created to allow accurate incorporation of collagen networks and solid matrix depth-dependent properties variation. The collagen fibrils were oriented horizontally parallel to the medial/lateral and anterior/posterior directions in the cartilage's superficial zone. In the transitional zone, the random fibrils (i.e., no dominant orientations) followed a gradual curvature, beginning with parallel orientations and turning perpendicular to the surface close to the deep zone. In the deep zone, vertical fibrils were primarily oriented normal to the subchondral junction. In menisci, element properties were oriented in the circumferential and radial directions, based on the local coordinate system's axes orientations. For more details of the model's development process, please see the ►**Supplementary Materials** (available online only) and our prior published studies.[35,37–40]

The aforementioned knee model has been updated with additional features and associated changes to develop the parametric FE model of biomechanical experiments which depict the ACL-R surgery. Accordingly, the model included tibial and femoral tunnels of 9 mm diameter with the exact geometry of BPTB graft, which was incorporated by separating the geometry of the graft from that of PT (►**Fig. 1**). Thereafter, a population of the models was created with respect to six intraoperative variables, two-quadrant coordinates of femoral tunnel placement, sagittal and coronal angles of the femoral tunnel, the graft tension, and the joint angle at which the BPTB graft is tensioned and fixed to the femoral tunnel (fixation angle) (►**Supplementary Fig. S1**) (For more details, please see ►**Supplementary Materials** [available online only]). A number of steps were adopted sequentially to conduct the surgical simulation; first, the proximal bone plug was placed inside the femoral tunnel, aligned with the tunnel axis. Second, the distal bone plug was placed and fixed in the tibial tunnel, with the proximal bone plug constraint to rotate and slide about the femoral tunnel axis. In the third simulation step, the tibia was flexed to a

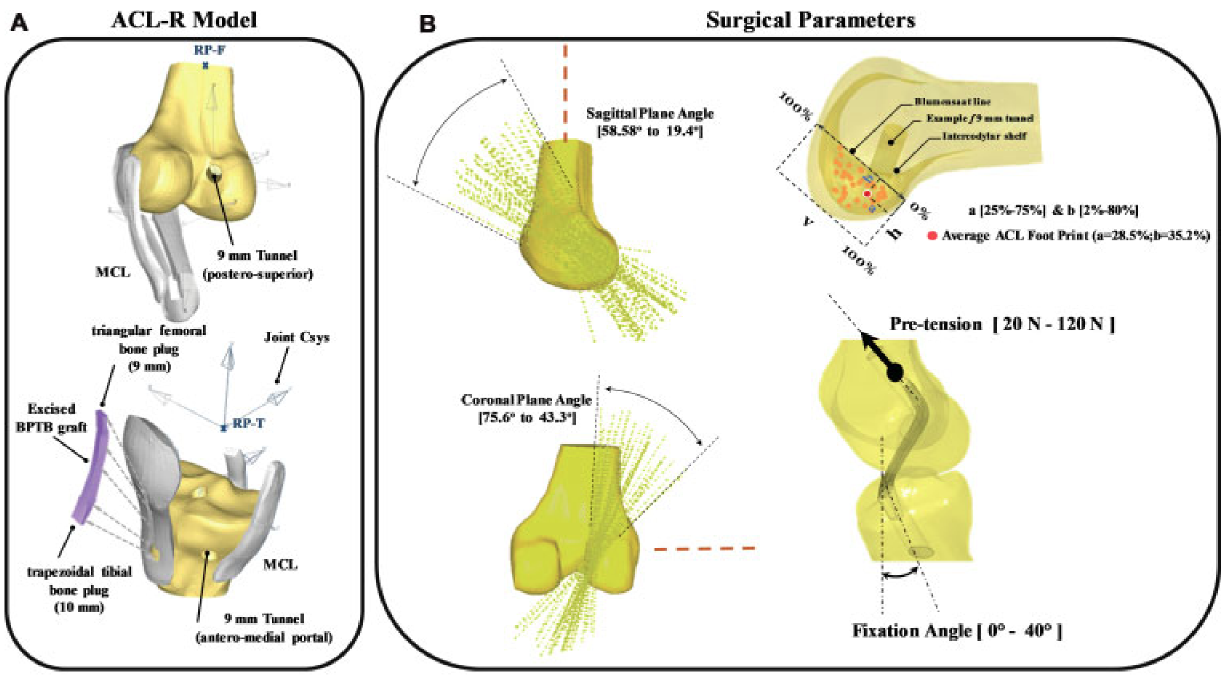

Fig. 1 (**A**) Anterior cruciate ligament reconstruction (ACL-R) model; reference point (RP)-T and RP-F are the reference nodes of the tibial and femoral bone, respectively; Joint Csys is the joint coordinate system. (**B**) Key geometrical aspects of the ACL-R surgery with the description of the considered range of tunnel directions, locations, fixation angle, and graft pretension. Details of the finite element (FE) model and the range of variation of the surgical parameters can be found in Dhaher et al[43] and ►**Supplementary Materials** (available in the online version only).

given fixation angle. Over the next step, the proximal bone plug was pulled along the femoral tunnel axis, using a given pretensioning force, keeping the tibia free in all degrees of freedom. Finally, the joint was fully extended, and the surgical simulation was completed (►**Supplementary Fig. S5** in the ►**Supplementary Materials** Section [available online only]). A subsequent simulation step was also introduced, where the knee joint was axially loaded under full extension by 1000 N to predict joint contact parameters. The femur was fixed under the applied compression force, while the tibia was left free, except the flexion-extension degree of freedom. All the boundary conditions were applied at the reference points (RP) of the femoral and tibial bones (►**Fig. 1A**). The observed similarity with the joint's load under single-leg standing activity,[41,42] the earlier validation and verification of the healthy model, and the achieved numerical convergence were the main motives behind the choice of 1000 N axial compression load.Detailed descriptions of the statistical calibration and validation of healthy and ACL-R models have been discussed in the ►**Supplementary Materials** (available online only) and our prior investigations.[33,34,43]

Material Properties

For the ligaments, a transversely isotropic hyperelastic material model assumed to be nearly incompressible and driven by an uncoupled representation of the strain energy function, as defined by Limbert and Middleton, was employed. In this framework, the fibers were assumed to be extensible and uniformly distributed in the ground substance and perfectly bonded to the matrix, while the matrix was assumed to be isotropic and hyperelastic. The menisci were considered as transversely isotropic, linearly elastic, and homogeneous material.[35] Multiplicative decomposition of the deformation gradient into elastic and plastic parts is introduced in the present work to create the fiber-reinforced composite model of cartilage. Therefore, a hierarchical hyperelastoplastic composite material starting from tropocollagen molecules level (300 nm) to continuum macrolevel (+100 µm) has been considered in the proposed model. Fundamentally, for soft tissues, the plastic flow is associated only with the uniaxial deformation of the collagen fibril.[45,46] Furthermore, the yield strength (g_0) of the fibril is a function of the cross-link density (β) between the tropocollagen molecules, defined herein by the density function g_0 (β). A coarse-graining procedure was employed to link the nanoscale collagen features and the tissue-level materials properties, using the cross-link density function as a building block. Neo-Hookean generalized strain energy was used to model the micro-fibrils, fibrils, and tissue behavior by considering the rule of mixtures. A 0.001 g/mm^3 density was assigned to all soft tissues,[47] while the rigid bony segments were assigned a density of 0.002 g/mm.[3,48] Details on the assigned materials' properties have been given in the ►**Supplementary Materials** (available online only) as well as our prior investigations.[35,37,38,40]

Sampling and Surrogate Modeling

The 6D space of surgical parameters was sampled using Maximin Latin hypercube sampling (LHS) algorithm. The sampling technique was considered to facilitate the addition of new training points to the formerly sampled space, in order to improve the precision of surrogate models. Reasonable bounds for the surgical parameters relative to data reported in a large body of the literature were employed. The parameter space was mapped using a radial basis function (RBF) to approximate the simulation response (contact parameters).[49] The minimum error of the RBF approximation was achieved with 48 training points.[33,34,43]

Probabilistic Sensitivity Analysis

The surrogate-based approach was employed to circumvent several executions of the computationally expensive ACL-R FE models during the probabilistic sensitivity analysis. Global sensitivity analysis based on variance decomposition, as described by Saltelli et al,[50] was employed to investigate the contributions of surgical parameters to the uncertainty in the response of the ACL-R joint. Hence, the contributions of a set of input parameters to the uncertainty in response output can be quantified by ranking the parameters, based on the output variance when one of the parameters is fixed to its true value. The expectation of all possible values of the input parameters was considered here to circumvent the surgical parameters' unknown true values (input parameters). Based on the above description, equation (1) has been used to determine the sensitivity indices[50] which is given by:

$$\sum_i S_i + \sum_i \sum_{j>i} S_{ij} + \cdots + S_{12\ldots6} = 1 \quad (1)$$

where S_i and Sij … are the first and the subsequent orders of sensitivities. These indices were calculated based on the following equations:

$$S_i = \frac{V\left(E(Y|X_i)\right)}{V(Y)} \quad (2)$$

$$S_{ij} = \frac{V\left(E(Y|X_i,X_j)\right) - V\left(E(Y|X_i)\right)}{V(Y)} \quad (3)$$

where X is the input parameters, Y is the output. V() and E() represent variance and expectation operators, respectively.

Results

Lower orientations of the femoral tunnel (coronal and sagittal) associated with a higher range of graft tensioning force have been observed as the two common factors within the two models characterized by a significant lateral compartmental contact force (►**Fig. 2A**). The majority of the surgical designs, that is, 26 out of 48 resulted in medial contact force magnitudes of 540 N ± 50N, which falls within the range of the healthy model prediction (►**Fig. 2B**). However, most of the designs that accommodate the augmentation of the medial contact force magnitude were characterized by more posterior-superior tunnel locations, higher graft tensioning, higher fixation angle (~ 35°) and femoral tunnel orientations ranging from 54° to 70° and from 36° to 55° in the coronal and sagittal planes, respectively. Nearly identical surgical parameters were assumed to be responsible for the increase of the total contact force (tunnel location, graft fixation angle, and tensioning force) (►**Fig. 2C**). We also observed that a higher range of graft tensioning force ranging from 85 to 116 N and a fixation angle ranging from 31° to 39° tend to shift the compartmental load distributions significantly from the lateral side to the medial side (►**Fig. 2D**).

The majority of the considered surgical designs resulted in a lower magnitude of total and compartmental contact areas than the intact model (►**Fig. 3**). A lower fixation angle (less than 14°) with a midrange tensioning force of nearly 60 ± 20 N led to contact areas almost equal to the contact area computed, considering the healthy model's same boundary conditions. We compared the contact center locations of 48 ACL-R models with the intact model, and it was observed that 5 out of the 48 models shifted the contact center laterally by more than 10% (►**Fig. 4B**). The fixation angle of the majority of these models ranged from 25° to 39° with similar femoral tunnel orientations (61 ± 8° and 45 ± 10° for coronal and sagittal angles, respectively) and a low range of graft tensioning force. Furthermore, the contact center also moved from the anterior to the posterior location with increasing graft pretensioning force (►**Fig. 4A**). An increase in the average contact pressure was evident in the majority of the surgical designs, among which the computed magnitude of 3 specific models (out of 48) reached approximately 1.60 MPa, which is twice the value of the intact model (►**Fig. 5A**). However, except for seven surgical designs, the rest of the designs resulted in maximum contact pressure within 30% of the intact model's calculated value (►**Fig. 5B**). The posterior location of the femoral tunnel associated with a higher graft fixation angle and a higher tensioning force led to a significant increase in the contact stress (►**Fig. 5**). Four out of the 48 models were selected at random to illustrate the contact pressure distributions at full extension and under axial compression of 1000 N (►**Fig. 6**). The surgical parameters for these models are shown in ►**Table 1**. The two samples (1 and 31) with a high-range tensioning force of 92/100 N experienced high maximum contact stress. A different list of 2D figures presetting the contact output as a function of a one-by-one surgical parameter was added to the ►**Supplementary Materials** (available online only) for additional access to the presented data.

Graft fixation angle and tensioning force were accounted for the most considerable parameters controlling the variance of the joint's total contact force (nearly 70%), among which 37% of the variance was due to the combined action of both parameters (fixation angle and tensioning force), 18% originated by the fixation angle, and the rest of 15% by the tensioning force. Tunnel placement was the second most crucial factor that accounted for 23% of the variance (►**Fig. 7**). The combined effect of the graft fixation angle and vertical tunnel location is primarily responsible for the variance (i.e., nearly 78%) in the contact area, whereas the fixation angle alone is responsible for 34% variance (►**Fig. 8**). However, the variance in the contact center shift was explained by the tunnel placement (46%) and followed by the graft fixation angle (34%) (►**Fig. 9**). Finally, it is found that both combined and individual changes in the graft tensioning force and fixation angle mainly control the sensitivity of the computed maximum contact stress (►**Fig. 10**).

Discussion

With reference to our prior computational studies on the effect of the critical surgical design parameters on the intra- and postoperative variables for a BPTB ACL-R

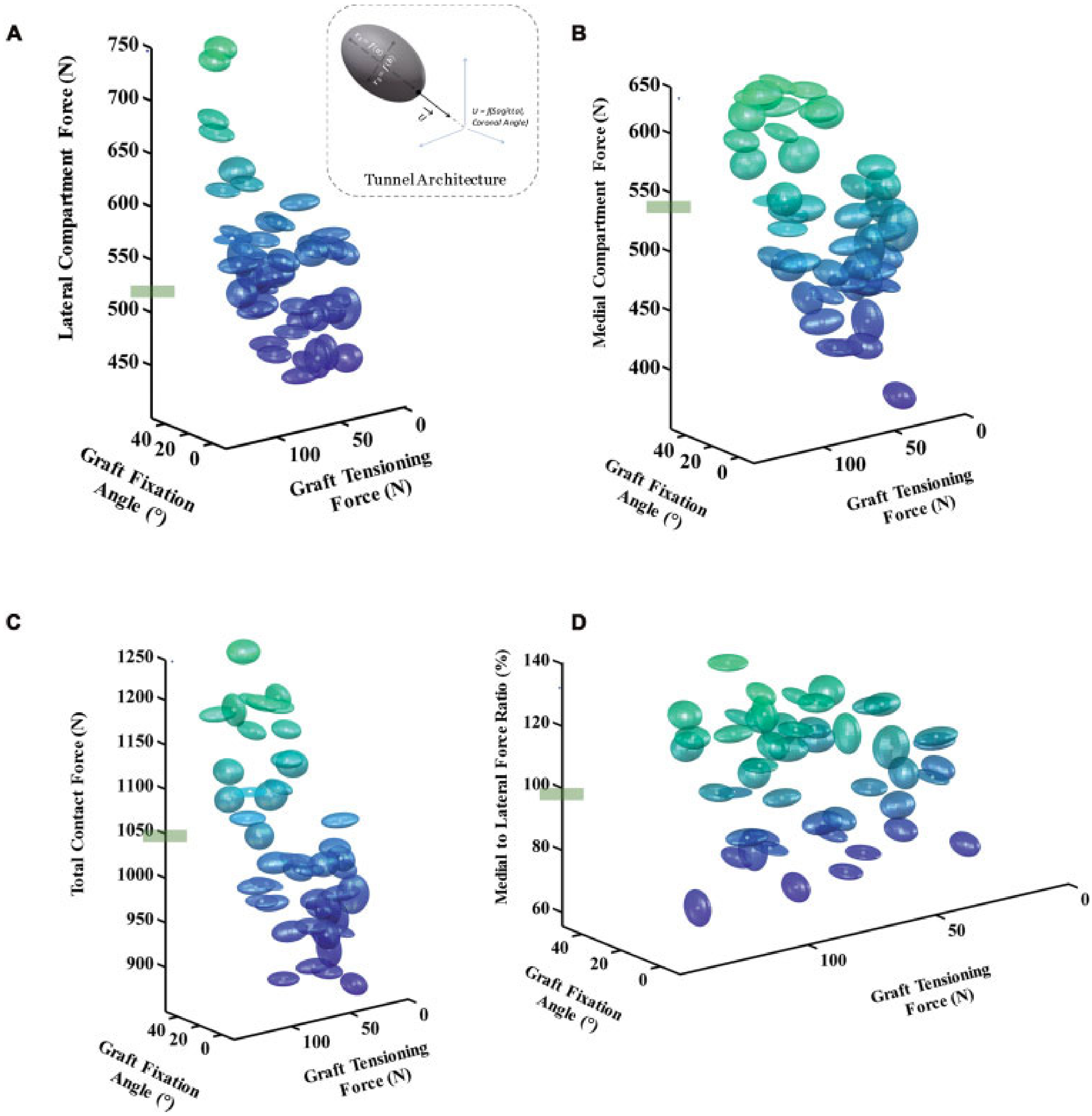

Fig. 2 The response of all 48 anterior cruciate ligament reconstruction (ACL-R) models constructed in this study are shown for the tibial contact force during an axial compression of 1000 N applied at full extension. (**A**) Lateral compartment force, (**B**) medial compartment force, (**C**) total compartment force, (**D**) medial to lateral contact force ratio. The shadow green line corresponds to contact behavior obtained from the healthy knee model under the same boundary conditions. Note, the x and y axes in the figures represent two of the surgical parameters (fixation angle and graft pretensioning force). Data points are represented in the gray dots located at the center of the ellipsoids in these figures. The ellipsoids associated with each of the data points represent the corresponding tunnel architecture. In this figure, the tunnel architecture is expressed in the form of an ellipsoid (see the inset) for which the principal direction is the three-dimensional direction of the tunnel and the size of the minor and major dimensions of the ellipsoid are in function of the quadrature coordinates of the tunnel placement (see ►**Fig. 1**). It is worth noting that the presented results' interpretation should be considered with certain care as it requests a complete knowledge of the inputs' set.

surgery, the current work aimed to investigate the effect of the surgical parameters on the articular contact behavior during axial knee compression.[43] The targeted outcomes are the joint's total and compartmental forces and areas, the contact center location, and the average and maximum contact stresses. Our analyses indicated that the variation in the tunnel's vertical location (anterior-posterior), the graft pretension, and the angle at the time of fixation accounted for most of the estimated variance of the knee articular contact behavior considered in the present work.

The contact force supported by the lateral compartment was found to increase significantly by almost 130 N to 215 N when the orientations of the femoral tunnel and the graft tensioning force were set nearly to the lower and upper bounds of the considered range of variations of these

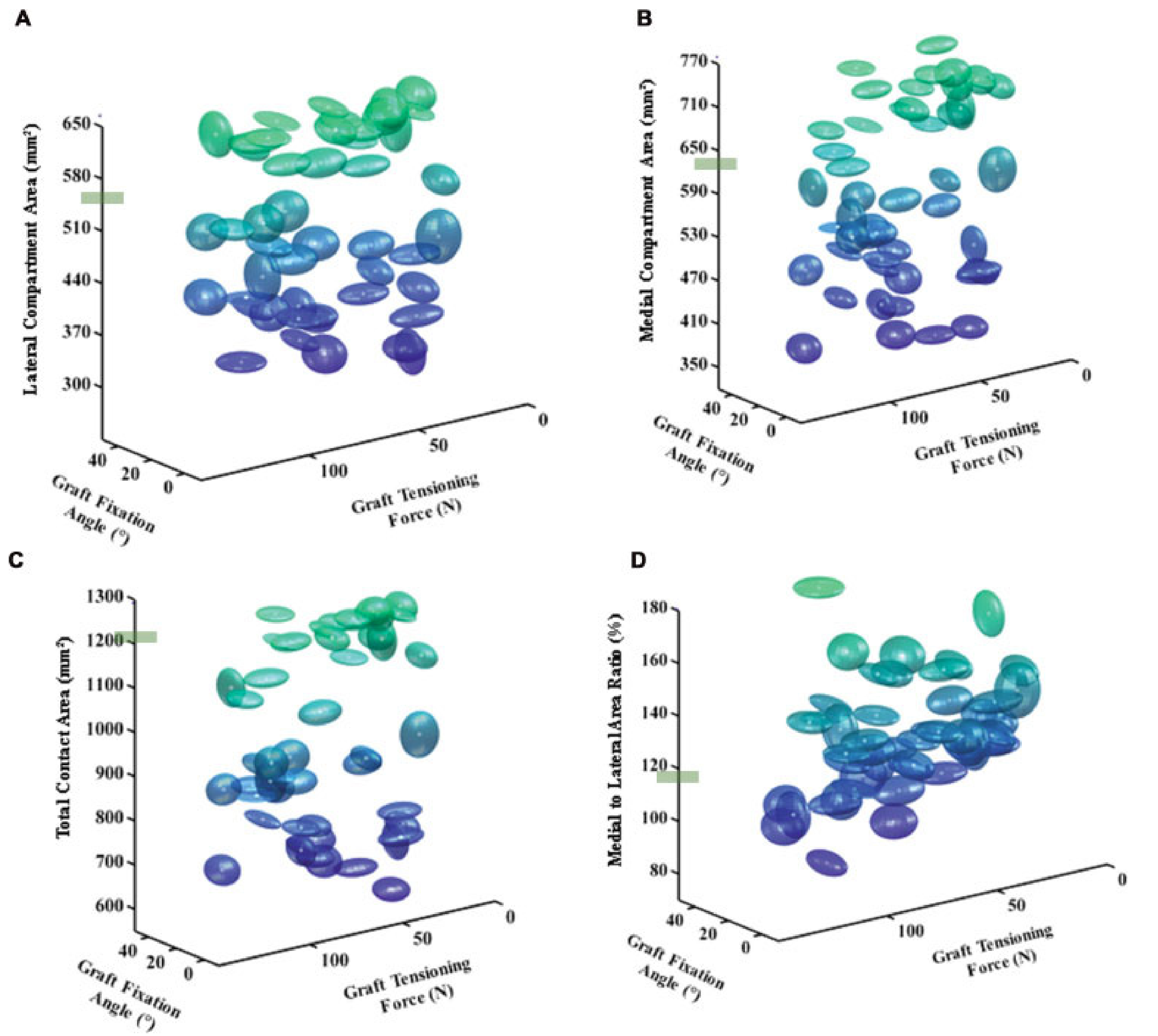

Fig. 3 The response of all 48 anterior cruciate ligament reconstruction (ACL-R) models constructed in this study are shown for the tibial contact area during an axial compression of 1000 N applied at full extension. (**A**) Lateral compartment area, (**B**) medial compartment area, (**C**) total compartment area, (**D**) medial to lateral contact area ratio. The shadow green line corresponds to the contact behavior obtained from the healthy knee model under the same boundary conditions.

parameters, that is, 19° on the sagittal plane, 43° on the coronal plane, and 120 N for the maximum graft tensioning force, respectively (►**Fig. 2A**). This augmentation may be attributed to the predicted and measured increase of the normal force at the tunnel-graft interface that was associated with lower tunnel angles and higher pretensioning graft force.[31,34,43,51] The orientation of this normal force seems to be responsible for the lateral increase in the knee compartmental load. However, the observed augmentation of the lateral compartmental load was associated with a slight decrease in the medial force ranging from 40 N to 80 N. The medial force was substantially decreased by nearly 34% when the surgery adopted a low graft pretensioning force (23 N), a low fixation angle (12°), and a low sagittal orientation of the femoral tunnel (28°), which were all associated with an anterior and inferior location of the tunnel (►**Fig. 2B**). It is worth mentioning that this design was characterized by a loose knee during the Lachman test,[43] an observation that was well corroborated by in vitro studies and mostly related to a low graft pretensioning force.[29,52–55] Only one model had higher compartmental loads of nearly 100 N on both the medial and lateral sides. This model was characterized by a high fixation angle of 38° and extreme superior-posterior tunnel locations (horizontal and vertical locations 22% and 28%, respectively). These findings suggest that the graft pretensioning force may not be the only factor contributing to the dramatic increase in the contact loading. The superior-posterior location of graft insertion and the high angle of fixation may also contribute to the aberrant contact force observed after the surgery. These earlier observations of the surgical design parameters' effect on the compartmental load distribution may help in designing optimal surgical procedures. These procedures may improve the kinematics and the kinetics of the unstable ACL-deficient knee with varus malalignment and medial compartment knee OA.[52,56] In other words, the double conservative

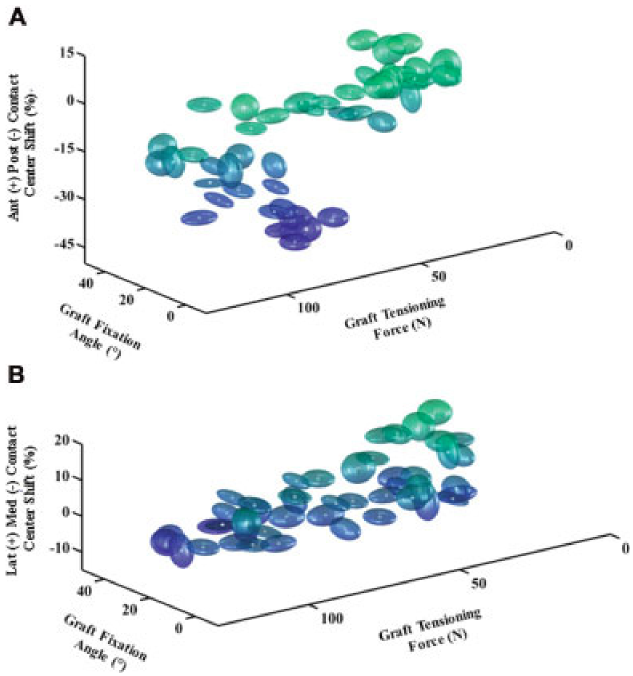

Fig. 4 The response of all 48 anterior cruciate ligament reconstruction (ACL-R) models constructed in this study are shown for the tibial contact center location shift relative to the contact center location obtained from the healthy knee model under the same boundary conditions (axial compression of 1000 N applied at full extension). The relative positions were normalized to the medial-lateral length and anteroposterior length.[69] (For more details, please see ►**Supplementary Materials Section**, available in the online version only). (**A**) Anterior and posterior contact center shift, (**B**) lateral and medial contact center shift.

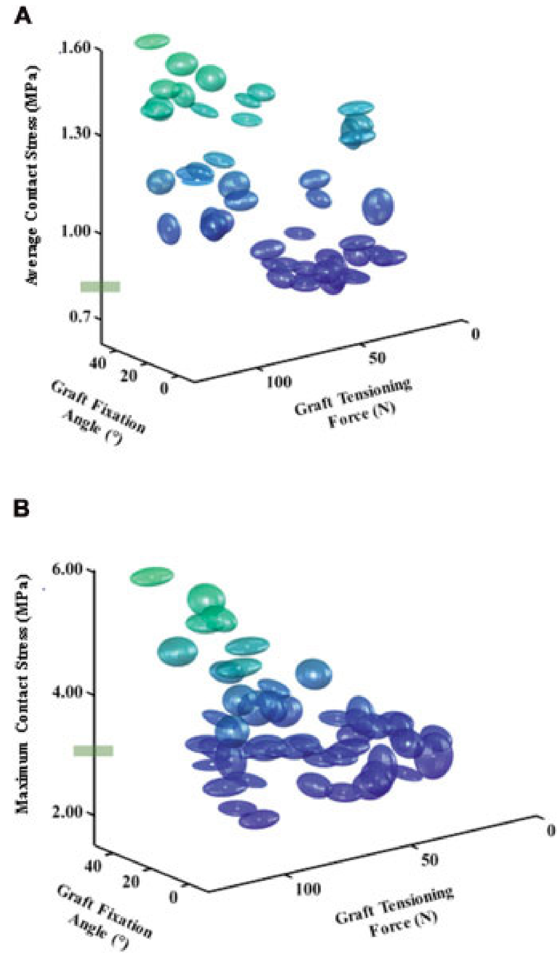

Fig. 5 The response of all 48 anterior cruciate ligament reconstruction (ACL-R) models constructed in this study are shown for the tibial contact stress during an axial compression of 1000 N applied at full extension. (**A**) Average contact stress, (**B**) maximum contact stress. The shadow green line corresponds to contact behavior obtained from the healthy knee model under the same boundary conditions.

corrections (ACL-R and knee osteotomy) may be replaced by one procedure (ACL-R).

Our results also indicated that a combination of specific surgical parameters might lead to a reconstructed total contact force of 1045 N, which is consistent with those computed for the intact joint when subjected to the same axial compression loading. More specifically, 8 out of 48 models exhibited a total contact force within 30 N (± 30 N) of that computed for the intact joint. However, 3 of these 8 models were characterized by an aberrant distribution of the compartmental load that differed more than 180 N between the tibial plateaus in the extreme case. These results suggest that the knee joint's total contact force should be carefully considered if it is used to evaluate the ability of ACL-R surgery, in order to restore the tibiofemoral contact behavior.[57–59] The compartmental and total forces of only one model fell within the range of the reported value of the intact model. For this particular model, the graft was fixed at 19° with a pretensioning force of 85 N, the femoral tunnel locations were 27% vertically and 13% horizontally, and the orientations were 48° coronal and 36° sagittal. This design successfully restored joint stability during the Lachman test but with a very high-stress concentration in the femoral graft-tunnel interface.[43] It is worth noting that the models with the lowest contact force values (898 N and 912 N) have been characterized mainly by a noticeable difference in their applied pretensioning force (71N and 23N) and vertical location (67% and 26%). Thus, a high graft pretensioning force associated with an anterior tunnel position (high vertical location) led to a minimum level of contact force. This observation is consistent with the findings reported in earlier published studies, indicating a loose reaction of the operated joint with low graft pretension or more anterior insertion of the tunnel.[29,52,54,60–63]

Most of the designs used in this investigation showed an apparent decrease in the contact area of the total and individual tibial plateaus (►**Fig. 3**). The decrease in the contact area in some of the models was as high as 50%, particularly in the medial plateau. Our contact area data was comparable to the results reported in a previous study using cadaveric knees.[23] An apparent decrease in the contact area is shown for a single-bundle ACL-R in comparison to both a double-bundle ACL-R case and an intact case. Unfortunately, it is essential to note that most of the models that have successfully restored the contact force fail to restore the contact area. For example, a reduction of almost 250 mm^2 of

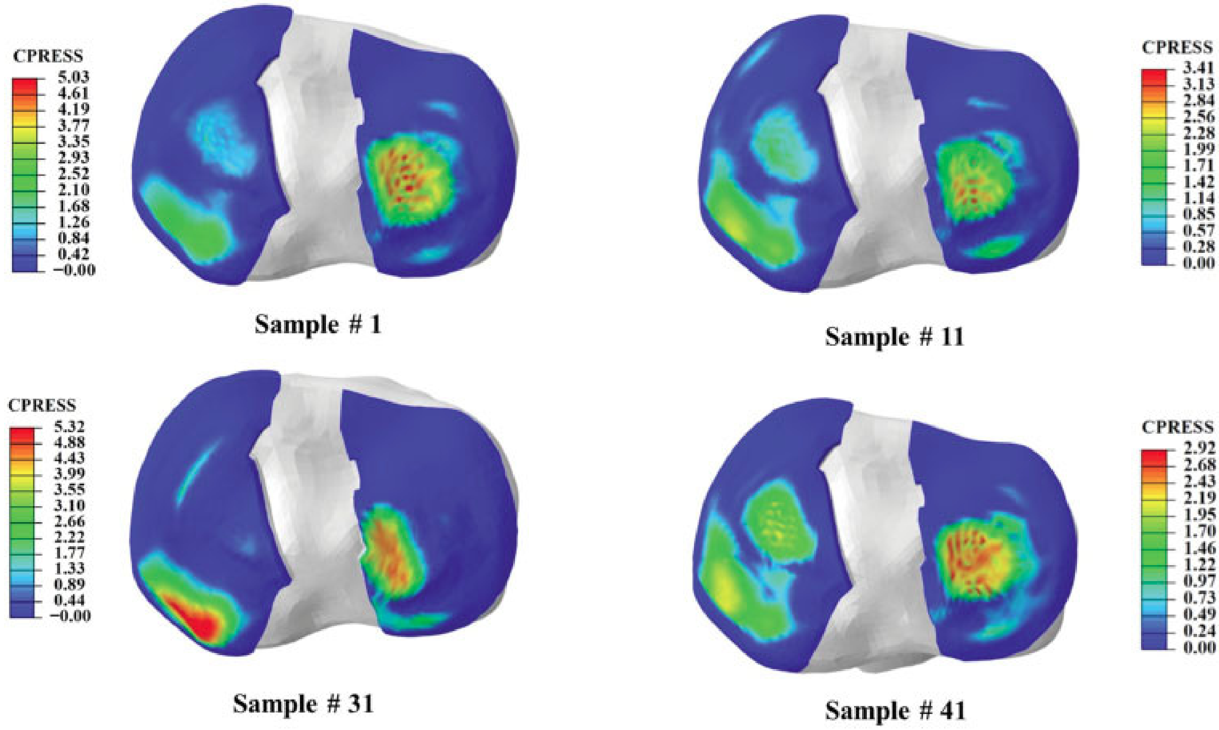

Fig. 6 Knee contact pressure distribution at full extension under 1000 N axial compression of four sample models selected at random from the 48 models constructed for this paper. ►**Table 1** provides the corresponding surgical design parameters for the selected samples.

Table 1 Surgical design parameters for the selected samples shown in ►**Fig. 6**

Sample number	Sagittal angle (°)	Coronal angle (°)	Horizontal quadrant coordinate (h%)	Vertical quadrant coordinate (v%)	Fixation angle (°)	Tensioning force (N)
1	28.23	74.67	6.98	33.85	6.25	92.99
11	26.87	48.75	38.85	63.53	17.83	50.21
31	46.08	53.33	12.05	29.63	30.42	100.62
41	32.75	68.28	46.05	61.12	25.08	39.79

the total contact area was computed with the design that most closely restored the knee to the intact contact force of 1045 N. However, only two models were nearly able to restore both the contact force and contact area properly. These models were characterized, respectively, by fixation angles of 14° and 11°, vertical locations of 49% and 33%, horizontal locations of 23% and 8%, coronal orientations of 46° and 56°, sagittal orientations of 27° and 48°, and pretensioning forces of 73 N and 36 N. Yet, these models increased the joint's laxity by approximately 50%, which was considered to be a significant limitation.[43] Furthermore, an apparent augmentation of the average and maximum contact stress was computed with most of the designs considered in this study. The stress concentration was localized more on the medial compartment than the lateral compartment. This result may be explained by the observed discrepancy between the force and the contact area, especially the aberrant decrease in the contact area of the medial compartment. Also, the common factors between all the models, which were characterized by 50% augmentation of the maximum contact stress, were the high values of the angle at which the graft was fixed and the graft pretension. It is important to note that, for some of the designs, even those with a lower contact force than the intact one, we computed approximately 30% (much) higher contact stress, which can be primarily explained by the alteration of the contact area. These earlier results may shed light on the association between knee cartilage degeneration and the decrease in the joint loading observed after ACL deficiency or ACL-R.[17,22,64]

In this study, our sensitivity analysis indicated that changes in the cross-terms (second orders indices) are more dominant than those in the first-order indices (►**Figs. 7–8910**). This observation emphasizes the importance of the interconnection between the surgical parameters that were considered during this investigation.[50] For

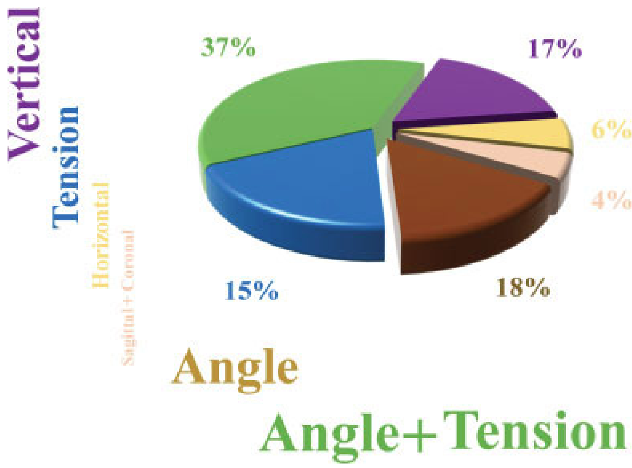

Fig. 7 Sensitivity indices (pie chart) based on the surrogate model prediction for the total tibial contact force in response to axial compression. The word cloud is a graphical representation of the sensitivity indices of the identified surgical parameters to the corresponding outcome. Sensitivity indices less than 1% were not displayed.

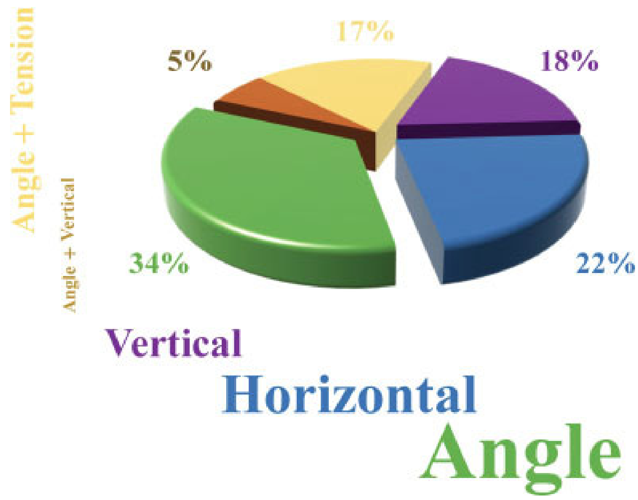

Fig. 9 Sensitivity indices (pie chart) based on the surrogate model prediction for the total tibial contact center location in response to axial compression. The word cloud is a graphical representation of the sensitivity indices of the identified surgical parameters to the corresponding outcome. Sensitivity indices less than 1% were not displayed.

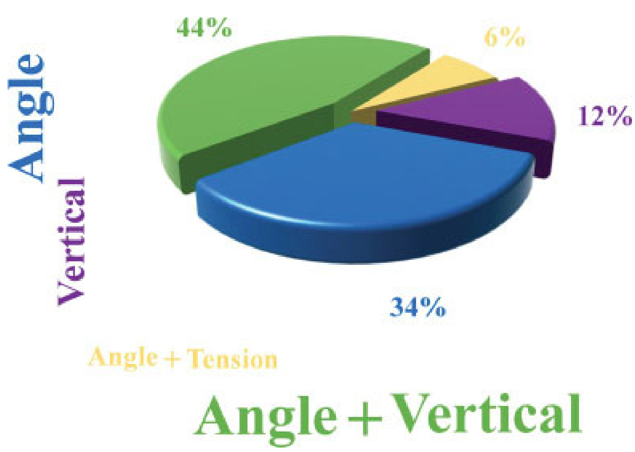

Fig. 8 Sensitivity indices (pie chart) based on the surrogate model prediction for the total tibial contact area in response to axial compression. The word cloud is a graphical representation of the sensitivity indices of the identified surgical parameters to the corresponding outcome. Sensitivity indices less than 1% were not displayed.

Fig. 10 Sensitivity indices (pie chart) based on the surrogate model prediction for the tibial contact maximum stress in response to axial compression. The word cloud is a graphical representation of the sensitivity indices of the identified surgical parameters to the corresponding outcome. Sensitivity indices less than 1% were not displayed.

example, the combined action of the graft pretension, vertical tunnel location, and sagittal tunnel orientation accounted for a significant portion of the variance (62%) in the lateral contact force. While the medial contact force was most sensitive to the tunnel location by a variability of 56%, it was mainly dominated by the combined variation in the horizontal and vertical sites (36%), followed by the vertical site only (20%). These observations suggest that femoral tunnel location and graft pretension have the most significant effect on the compartmental load distributions that could lead to an aberrant load on the medial side or lateral side; hence, leading to the potential of cartilage degeneration.[25,29] However, with earlier surgical parameters affecting the compartmental load distribution, the fixation angle was considered to be the additional principal factor contributing to the total contact force variability (only the sensitivity of the total contact force was presented here). This result is consistent with the findings reported by Mae et al,[30] who observed a stiffer postoperative joint with the augmentation of the angle of fixation.The combined action of tunnel location and fixation angle contributed to the variability of the area and the center of the contact by 84% and 91%, respectively. The sensitivity of the articular cartilage's maximum contact stress, which is considered to be an essential predictor of cartilage damage initiation and propagation, was mostly affected by the graft pretension and fixation angle (86% of variability). This variability was dominated by the graft pretension (31%), followed by the fixation angle (28%), and then by their combined action (27%). It is interesting to note that the fixation angle, the tunnel locations, and graft pretension were the most common surgical parameters affecting the tibiofemoral contact behavior. However, this behavior was almost insensitive to the tunnel's coronal and sagittal orientations, except for the case of the lateral compartment load. These findings highlight the complexity associated with the restoration of knee joint contact behavior after ACL-R surgery. Additionally, such observation may explain the well-documented evidence of posttraumatic cartilage degradation.[9,10]

The computational framework and the outcomes of the current work are circumscribed by a few limitations. First, only one joint loading scenario was simulated during the investigation. Second, the capsular ligament around the knee joint was not considered in the knee model. Third, hyperelastic behavior was used as a proxy of the soft tissues' biphasic behavior in the model. However, this proxy has been well-documented as an approved tool to accurately capture the transient response of soft tissue.[65] Fourth, the ACL-R models do not consider structural changes (tunnel expansion) or changes in the contact properties, either in the interface of the tunnel-graft area or within the tibiofemoral joint. While graft remodeling and cycling loading can change the initial stress within the graft over time,[66] in the present study, the wide range of initial pretension values (20 N to 120 N) included possible graft tensions at different time intervals postoperatively; hence, the findings gleaned from the current sensitivity analysis can be generalized to postsurgical states. Moreover, the current model did not account for the potential posterior tibial sag attributed to the patient's intraoperative supine posture, a posterior displacement that may affect the joint's kinematics after the surgery.[67] Finally, this study did not consider muscles. However, incorporating these components may improve the accuracy of the simulation of the daily activities of the knee joint and rehabilitation treatments.[68]

In conclusion, the current investigation used a systematic engineering approach to assess the relative influence of the surgical design parameters associated with ACL-R surgery on postoperative knee joint contact mechanics. To the best of our knowledge, this is the first model ever published in which the surgery outcomes are computed as a function of the simultaneous interaction of a high number of surgical factors (six factors). The results provide an evaluation of how the surgical parameters can affect a knee joint's contact behavior after an ACL-R. This evaluation shows the clear differences in contact behavior during axial compression in ACL-R knees in comparison to a normal knee. The contact alterations may relate to the high incidence of knee OA observed in this population over time. In the context of the design of prospective studies, our findings evaluate the ACL-R surgery variables to restore the articular contact parameters by highlighting the importance of the tunnel's placement, graft pretension, and flexion angle at the time of fixation.

Authors' Contributions
All authors have read and approved this submission. The first author carried out analyses. All participated in the definition, design, and development of the work. Finally, the manuscript was written by all authors.

Funding
This work is supported by a grant (#U01 EB015410-01A1) from the National Institute of Health NIH.

Conflict of Interest
None declared.

References

1 Shelton WR, Fagan BC. Autografts commonly used in anterior cruciate ligament reconstruction. J Am Acad Orthop Surg 2011;19 (05):259–264
2 Abram SGF, Price AJ, Judge A, Beard DJ. Anterior cruciate ligament (ACL) reconstruction and meniscal repair rates have both increased in the past 20 years in England: hospital statistics from 1997 to 2017. Br J Sports Med 2020;54(05):286–291
3 Zbrojkiewicz D, Vertullo C, Grayson JE. Increasing rates of anterior cruciate ligament reconstruction in young Australians, 2000-2015. Med J Aust 2018;208(08):354–358
4 Tashman S, Kolowich P, Collon D, Anderson K, Anderst W. Dynamic function of the ACL-reconstructed knee during running. Clin Orthop Relat Res 2007;454(454):66–73
5 Biau DJ, Tournoux C, Katsahian S, Schranz P, Nizard R. ACL reconstruction: a meta-analysis of functional scores. Clin Orthop Relat Res 2007;458(458):180–187
6 Fithian DC, Paxton EW, Stone ML, et al. Prospective trial of a treatment algorithm for the management of the anterior cruciate ligament-injured knee. Am J Sports Med 2005;33(03):335–346
7 Lohmander LS, Östenberg A, Englund M, Roos H. High prevalence of knee osteoarthritis, pain, and functional limitations in female soccer players twelve years after anterior cruciate ligament injury. Arthritis Rheum 2004;50(10):3145–3152
8 Lohmander LS, Gerhardsson de Verdier M, Rollof J, Nilsson PM, Engström G. Incidence of severe knee and hip osteoarthritis in relation to different measures of body mass: a population-based prospective cohort study. Ann Rheum Dis 2009;68(04): 490–496
9 Paschos NK. Anterior cruciate ligament reconstruction and knee osteoarthritis. World J Orthop 2017;8(03):212–217
10 Paschos NK, Howell SM. Anterior cruciate ligament reconstruction: principles of treatment. EFORT Open Rev 2017;1(11): 398–408
11 Nakamura N, Zaffagnini S, Marx RG, Musahl V. Controversies in the Technical Aspects of ACL Reconstruction: An Evidence-Based Medicine Approach. Berlin, Germany: Springer; 2017
12 Bush-Joseph CA, Hurwitz DE, Patel RR, et al. Dynamic function after anterior cruciate ligament reconstruction with autologous patellar tendon. Am J Sports Med 2001;29(01):36–41
13 Georgoulis AD, Papadonikolakis A, Papageorgiou CD, Mitsou A, Stergiou N. Three-dimensional tibiofemoral kinematics of the anterior cruciate ligament-deficient and reconstructed knee during walking. Am J Sports Med 2003;31(01):75–79
14 Georgoulis AD, Ristanis S, Chouliaras V, Moraiti C, Stergiou N. Tibial rotation is not restored after ACL reconstruction with a hamstring graft. Clin Orthop Relat Res 2007;454(454):89–94
15 Van de Velde SK, Gill TJ, DeFrate LE, Papannagari R, Li G. The effect of anterior cruciate ligament deficiency and reconstruction on the patellofemoral joint. Am J Sports Med 2008;36(06): 1150–1159
16 Webster KE, Feller JA. Alterations in joint kinematics during walking following hamstring and patellar tendon anterior cruciate ligament reconstruction surgery. Clin Biomech (Bristol, Avon) 2011;26(02):175–180

17 Zabala ME, Favre J, Scanlan SF, Donahue J, Andriacchi TP. Three-dimensional knee moments of ACL reconstructed and control subjects during gait, stair ascent, and stair descent. J Biomech 2013;46(03):515–520
18 Hsieh Y-F, Draganich LF, Ho SH, Reider B. The effects of removal and reconstruction of the anterior cruciate ligament on patellofemoral kinematics. Am J Sports Med 1998;26(02): 201–209
19 Stergiou N, Ristanis S, Moraiti C, Georgoulis AD. Tibial rotation in anterior cruciate ligament (ACL)-deficient and ACL-reconstructed knees: a theoretical proposition for the development of osteoarthritis. Sports Med 2007;37(07):601–613
20 Mesfar W, Shirazi-Adl A. Biomechanics of changes in ACL and PCL material properties or prestrains in flexion under muscle force-implications in ligament reconstruction. Comput Methods Biomech Biomed Engin 2006;9(04):201–209
21 Halonen KS, Mononen ME, Töyräs J, Kröger H, Joukainen A, Korhonen RK. Optimal graft stiffness and pre-strain restore normal joint motion and cartilage responses in ACL reconstructed knee. J Biomech 2016;49(13):2566–2576
22 Saxby DJ, Bryant AL, Modenese L, et al. Tibiofemoral contact forces in the anterior cruciate ligament-reconstructed knee. Med Sci Sports Exerc 2016;48(11):2195–2206
23 Morimoto Y, Ferretti M, Ekdahl M, Smolinski P, Fu FH. Tibiofemoral joint contact area and pressure after single- and double-bundle anterior cruciate ligament reconstruction. Arthroscopy 2009;25(01):62–69
24 Wang L, Lin L, Feng Y, et al. Anterior cruciate ligament reconstruction and cartilage contact forces–A 3D computational simulation. Clin Biomech (Bristol, Avon) 2015;30(10):1175–1180
25 Westermann RW, Wolf BR, Elkins J. Optimizing graft placement in anterior cruciate ligament reconstruction: A finite element analysis. J Knee Surg 2017;30(02):97–106
26 Koga H, Muneta T, Yagishita K, et al. Effect of posterolateral bundle graft fixation angles on graft tension curves and load sharing in double-bundle anterior cruciate ligament reconstruction using a transtibial drilling technique. Arthroscopy 2013;29 (03):529–538
27 Koga H, Muneta T, Yagishita K, et al. Effect of posterolateral bundle graft fixation angles on clinical outcomes in double-bundle anterior cruciate ligament reconstruction: a randomized controlled trial. Am J Sports Med 2015;43(05):1157–1164
28 Kondo E, Yasuda K, Kitamura N, et al. Effects of initial graft tension on clinical outcome after anatomic double-bundle anterior cruciate ligament reconstruction: comparison of two graft tension protocols. BMC Musculoskelet Disord 2016;17(01):65
29 Mae T, Shino K, Nakata K, Toritsuka Y, Otsubo H, Fujie H. Optimization of graft fixation at the time of anterior cruciate ligament reconstruction. Part I: effect of initial tension. Am J Sports Med 2008;36(06):1087–1093
30 Mae T, Shino K, Nakata K, Toritsuka Y, Otsubo H, Fujie H. Optimization of graft fixation at the time of anterior cruciate ligament reconstruction. Part II: effect of knee flexion angle. Am J Sports Med 2008;36(06):1094–1100
31 Peña E, Calvo B, Martinez MA, Palanca D, Doblaré M Influence of the tunnel angle in ACL reconstructions on the biomechanics of the knee joint. Clin Biomech (Bristol, Avon) 2006;21(05): 508–516
32 van Kampen A, Wymenga AB, van der Heide HJ, Bakens HJ. The effect of different graft tensioning in anterior cruciate ligament reconstruction: a prospective randomized study. Arthroscopy 1998;14(08):845–850
33 Salehghaffari S, Dhaher YY. A model of articular cruciate ligament reconstructive surgery: a validation construct and computational insights. J Biomech 2014;47(07):1609–1617
34 Salehghaffari S, Dhaher YY. A phenomenological contact model: understanding the graft-tunnel interaction in anterior cruciate ligament reconstructive surgery. J Biomech 2015;48(10):1844–1851
35 Adouni M, Faisal TR, Gaith M, Dhaher YY. A multiscale synthesis: characterizing acute cartilage failure under an aggregate tibiofemoral joint loading. Biomech Model Mechanobiol 2019;18(06): 1563–1575
36 Andriacchi TP, Dyrby CO. Interactions between kinematics and loading during walking for the normal and ACL deficient knee. J Biomech 2005;38(02):293–298
37 Dhaher YY, Kwon TH, Barry M. The effect of connective tissue material uncertainties on knee joint mechanics under isolated loading conditions. J Biomech 2010;43(16):3118–3125
38 Adouni M, Dhaher YY. A multi-scale elasto-plastic model of articular cartilage. J Biomech 2016;49(13):2891–2898
39 Barry MJ, Kwon T-H, Dhaher YY. Probabilistic musculoskeletal modeling of the knee: A preliminary examination of an ACL-reconstruction. Paper presented at: Engineering in Medicine and Biology Society (EMBC) Annual International Conference of the IEEE2010, Buenos Aires, Argentina2010
40 Faisal TR, Adouni M, Dhaher YY. The effect of fibrillar degradation on the mechanics of articular cartilage: a computational model. Biomech Model Mechanobiol 2019;18(03):733–751
41 Harrison EL, Duenkel N, Dunlop R, Russell G. Evaluation of single-leg standing following anterior cruciate ligament surgery and rehabilitation. Phys Ther 1994;74(03):245–252
42 Noyes SB-WDF. ACL Injury Rehabilitation: Everything You Need to Know to Restore Knee Function and Return to Activity. Cincinnati, United States: Noyes Knee Institute; 2012
43 Dhaher YY, Salehghaffari S, Adouni M. Anterior laxity, graft-tunnel interaction and surgical design variations during anterior cruciate ligament reconstruction: A probabilistic simulation of the surgery. J Biomech 2016;49(13):3009–3016
44 Limbert G, Middleton J. A transversely isotropic viscohyperelastic material: Application to the modeling of biological soft connective tissues. Int J Solids Struct 2004;41(15):4237–4260
45 Tang H, Buehler MJ, Moran B. A constitutive model of soft tissue: from nanoscale collagen to tissue continuum. Ann Biomed Eng 2009;37(06):1117–1130
46 Tang Y, Ballarini R, Buehler MJ, Eppell SJ. Deformation micromechanisms of collagen fibrils under uniaxial tension. J R Soc Interface 2010;7(46):839–850
47 Penrose JM, Holt GM, Beaugonin M, Hose DR. Development of an accurate three-dimensional finite element knee model. Comput Methods Biomech Biomed Engin 2002;5(04):291–300
48 Hoffer MM. A primer of orthopaedic biomechanics. JAMA 1983; 249(17):2397
49 Fang H, Rais-Rohani M, Liu Z, Horstemeyer M. A comparative study of metamodeling methods for multiobjective crashworthiness optimization. Comput Struc 2005;83(25–26):2121–2136
50 Saltelli A, Annoni P, Azzini I, Campolongo F, Ratto M, Tarantola S. Variance based sensitivity analysis of model output. Design and estimator for the total sensitivity index. Comput Phys Commun 2010;181(02):259–270
51 Segawa H, Koga Y, Omori G, Sakamoto M, Hara T. Influence of the femoral tunnel location and angle on the contact pressure in the femoral tunnel in anterior cruciate ligament reconstruction. Am J Sports Med 2003;31(03):444–448
52 Markolf KL, Hame S, Hunter DM, et al. Effects of femoral tunnel placement on knee laxity and forces in an anterior cruciate ligament graft. J Orthop Res 2002;20(05):1016–1024
53 Arnold MP, Lie DTT, Verdonschot N, de Graaf R, Amis AA, van Kampen A. The remains of anterior cruciate ligament graft tension after cyclic knee motion. Am J Sports Med 2005;33(04):536–542
54 Amis AA, Jakob RP. Anterior cruciate ligament graft positioning, tensioning and twisting. Knee Surg Sports Traumatol Arthrosc 1998;6(01, Suppl 1):S2–S12
55 Yasuda K, Tsujino J, Tanabe Y, Kaneda K. Effects of initial graft tension on clinical outcome after anterior cruciate ligament reconstruction. Autogenous doubled hamstring tendons connected in series with polyester tapes. Am J Sports Med 1997;25(01):99–106

56 Herman BV, Giffin JR. High tibial osteotomy in the ACL-deficient knee with medial compartment osteoarthritis. J Orthop Traumatol 2016;17(03):277–285
57 Jordan MJ, Aagaard P, Herzog W. Lower limb asymmetry in mechanical muscle function: A comparison between ski racers with and without ACL reconstruction. Scand J Med Sci Sports 2015;25(03):e301–e309
58 Sanford BA, Williams JL, Zucker-Levin AR, Mihalko WM. Tibiofemoral joint forces during the stance phase of gait after ACL reconstruction. Open J Biophys 2013;3(04):8
59 Tsai LC, McLean S, Colletti PM, Powers CM. Greater muscle co-contraction results in increased tibiofemoral compressive forces in females who have undergone anterior cruciate ligament reconstruction. J Orthop Res 2012;30(12):2007–2014
60 Garofalo R, Moretti B, Kombot C, Moretti L, Mouhsine E. Femoral tunnel placement in anterior cruciate ligament reconstruction: rationale of the two incision technique. J Orthop Surg Res 2007; 2:10–10
61 Kaseta MK, DeFrate LE, Charnock BL, Sullivan RT, Garrett WE Jr. Reconstruction technique affects femoral tunnel placement in ACL reconstruction. Clin Orthop Relat Res 2008;466(06):1467–1474
62 Plaweski S, Cazal J, Rosell P, Merloz P. Anterior cruciate ligament reconstruction using navigation: a comparative study on 60 patients. Am J Sports Med 2006;34(04):542–552
63 Pearle AD, McAllister D, Howell SM. Rationale for strategic graft placement in anterior cruciate ligament reconstruction: I.D.E.A.L. femoral tunnel position. Am J Orthop 2015;44(06):253–258
64 Konrath JM, Saxby DJ, Killen BA, et al. Muscle contributions to medial tibiofemoral compartment contact loading following ACL reconstruction using semitendinosus and gracilis tendon grafts. PLoS One 2017;12(04):e0176016
65 Ateshian GA, Ellis BJ, Weiss JA. Equivalence between short-time biphasic and incompressible elastic material responses. J Biomech Eng 2007;129(03):405–412
66 Graf BK, Henry J, Rothenberg M, Vanderby R. Anterior cruciate ligament reconstruction with patellar tendon. An ex vivo study of wear-related damage and failure at the femoral tunnel. Am J Sports Med 1994;22(01):131–135
67 Nakamura N, Zaffagnini S, Marx RG, Musahl V. Controversies in the Technical Aspects of ACL Reconstruction. Berlin HeidelbergSpringer2017
68 Schroeder MJ. A Multi-Domain Synthesis of Neuromechanical Adaptations Post Anterior Cruciate Ligament Reconstructive Surgery. Evanston, Illinois: Biomedical Engineering, Northwestern University; 2014
69 Zhang Y, Chen Y, Qiang M, et al. Comparison between three-dimensional CT and conventional radiography in proximal tibia morphology. Medicine (Baltimore) 2018;97(30):e11632

